

# Chemical Science

Accepted Manuscript



This article can be cited before page numbers have been issued, to do this please use: Y. Kita, T. Yata, Y. Nishimoto, K. Chiba and M. Yasuda, *Chem. Sci.*, 2018, DOI: 10.1039/C8SC01537F.



This is an Accepted Manuscript, which has been through the Royal Society of Chemistry peer review process and has been accepted for publication.

Accepted Manuscripts are published online shortly after acceptance, before technical editing, formatting and proof reading. Using this free service, authors can make their results available to the community, in citable form, before we publish the edited article. We will replace this Accepted Manuscript with the edited and formatted Advance Article as soon as it is available.

You can find more information about Accepted Manuscripts in the [author guidelines](#).

Please note that technical editing may introduce minor changes to the text and/or graphics, which may alter content. The journal's standard [Terms & Conditions](#) and the ethical guidelines, outlined in our [author and reviewer resource centre](#), still apply. In no event shall the Royal Society of Chemistry be held responsible for any errors or omissions in this Accepted Manuscript or any consequences arising from the use of any information it contains.

# Selective Oxymetalation of Terminal Alkynes via 6-*Endo* Cyclization: Mechanistic Investigation and Application to the Efficient Synthesis of 4-Substituted Isocoumarins

Yuji Kita,<sup>a</sup> Tetsuji Yata,<sup>a</sup> Yoshihiro Nishimoto,<sup>\*b</sup> Kouji Chiba<sup>c</sup> and Makoto Yasuda<sup>\*a</sup>

Received 00th January 20xx,  
Accepted 00th January 20xx

DOI: 10.1039/x0xx00000x

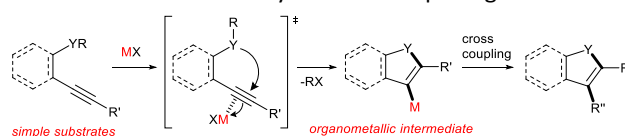
www.rsc.org/

Cyclization of heteroatom-containing alkynes with  $\pi$  acidic metal salts is an attractive method to prepare heterocycles because the starting materials are readily available and the organometallic compounds are useful synthetic intermediates. A new organometallic species in heterocyclization provides an opportunity to synthesize heterocycles that are difficult to obtain. Herein, we describe a novel cyclic oxymetalation of 2-alkynylbenzoate with indium or gallium salts that proceeds with an unusual regioselectivity to give isocoumarins bearing a carbon-metal bond at the 4-position. This new type of metalated isocoumarins provided 3-unsubstituted isocoumarins that have seldom been investigated despite their important pharmacological properties. Indium and gallium salts showed high performance in the selective 6-*endo* cyclization of terminal alkynes while boron or the other metals such as Al, Au, Ag caused 5-*exo* cyclization or decomposition of terminal alkynes, respectively. Metalated isocoumarin and its reaction intermediate were unambiguously identified by X-ray crystallographic analysis. Theoretical calculation of potential energy profiles showed that oxyindation could proceed via 6-*endo* cyclization under thermodynamic control while previously reported oxyboration would give a 5-membered ring under kinetic control. Investigation of electrostatic potential maps suggested that the differences in the atomic characters of indium, boron and their ligands would contribute to such a regioselective switch. The metalated isocoumarins were applied to organic synthetic reactions. Halogenation of metalated isocoumarins proceeded to afford 4-halogenated isocoumarins bearing various functional groups. The palladium-catalyzed cross coupling of organometallic species with organic halides gave various 4-substituted isocoumarins. A formal total synthesis of oosponol, which exhibits strong antifungal activity, was accomplished.

## Introduction

Heterocyclic compounds have attracted much attention in pharmaceutical chemistry as well as in photochemistry, and also play a pivotal role as building blocks in organic synthetic transformation.<sup>1</sup> Therefore, a novel efficient synthetic method for heterocyclic frameworks is highly desired in various fields of chemistry. Many well-established methods are available in the literature.<sup>2</sup> Heterocyclization of  $\omega$ -heteroatom-substituted alkynes using  $\pi$  acidic metal salts is undoubtedly a powerful strategy for the preparation of heterocycles (Scheme 1).<sup>3</sup> This addition reaction uses readily available alkynes as a starting material. Furthermore, metal salt-mediated cyclization

spontaneously forms a carbon-metal bond and a heterocyclic framework and produces organometallic intermediates leading to target heterocycles via appropriate synthetic reactions such as cross coupling. These features allowed us to directly access various substituted heterocycles from simple organic substrates.



**Scheme 1** Metal Salt-Mediated Heterocyclization of  $\omega$ -Heteroatom-substituted Alkynes.

Various heteroatom-containing alkynes have been investigated for use in the synthesis of heterocyclic compounds using  $\pi$  acidic metal salts. Alkyne **A** includes a carbonyl moiety and is a feasible and beneficial substrate to obtain 5- or 6-membered oxacyclic alkenylmetals (Scheme 2A). When **A** is treated with a metal salt (MX), oxymetalation proceeds to afford heterocyclic compounds through either 5-*exo* or 6-*endo* cyclization (Type *exo* or *endo*). Considering that the structure of **A** bears either an internal ( $R$  = alkyl, aryl etc.) or a terminal alkyne ( $R$  = H), oxymetalation can be distinguished by four types of reaction courses: Type *exo*-i, Type *exo*-t, Type *endo*-i, and Type *endo*-t. In Type *exo*-i and *exo*-t, the furan frameworks **B**

<sup>a</sup> Department of Applied Chemistry, Graduate School of Engineering, Osaka University, 2-1 Yamadaoka, Suita, Osaka 565-0871, Japan. E-mail: yasuda@chem.eng.osaka-u.ac.jp

<sup>b</sup> Frontier Research Base for Global Young Researchers Center for Open Innovation Research and Education (COiRE), Graduate School of Engineering, Osaka University, 2-1 Yamadaoka, Suita, Osaka 565-0871, Japan. E-mail: nishimoto@chem.eng.osaka-u.ac.jp

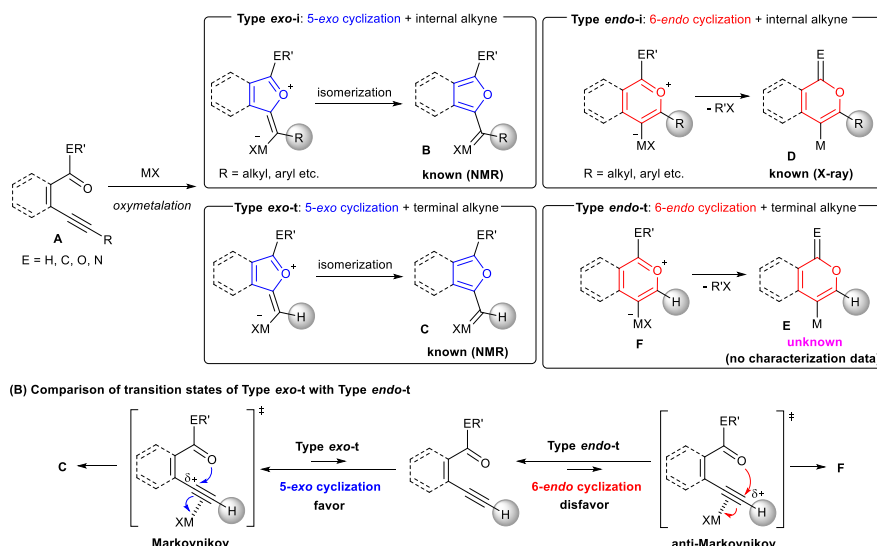
<sup>c</sup> Material Science Division, MOLSIS Inc., 1-28-38 Shinkawa, Chuo-ku, Tokyo 104-0033, Japan.

† Electronic Supplementary Information (ESI) available: Additional experimental data, characterization, calculation data and experimental details. See DOI: 10.1039/x0xx00000x



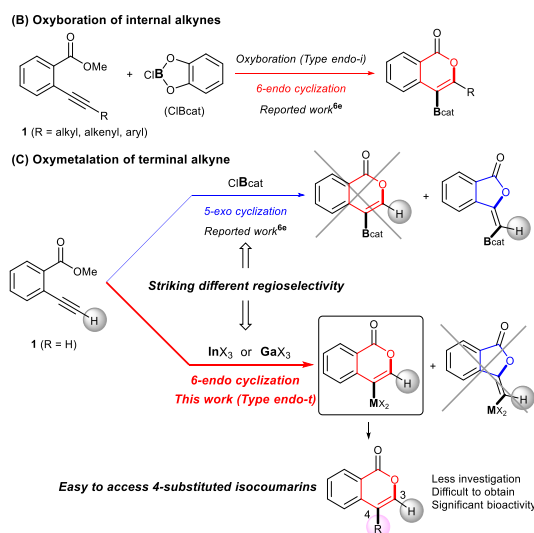
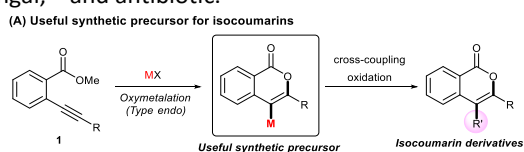
and **C** have a metal carbenoid moiety and are obtained via the isomerization of zwitterion intermediates.<sup>4,5</sup> On the other hand, Type *endo-i* and *endo-t* lead to 1*H*-isochromen derivatives **D** and **E** via elimination of R'X from zwitterion intermediates.<sup>6,7</sup> Among these four types, only Type *endo-t* is kinetically unfavorable due to an unstable cationic transition state via an *anti*-Markovnikov addition manner (Scheme 2B). Furthermore, recent theoretical researches about the regioselectivity of cyclization revealed that nucleophilic cyclization of alkynes displays *exo* selectivity intrinsically.<sup>8</sup> On the other hand, Lewis acidic metals can promote *endo* cyclization by decrease of the stereoelectronic

penalty, but the *exo* cyclization was not disturbed, and thus, the cyclization showed low selectivity.<sup>7,9</sup> For the above reasons, there is no report of a preparation method for species **E** via Type *endo-t* in contrast to the cases of Types *exo-i*, *exo-t*, and *endo-i*, for which target organometallic compounds (**B**, **C**, **D**) are well established.<sup>4b,5a,6c,6e</sup> If the reaction course of oxymetalation is realized from **A** to **E** in Type *endo-t*,<sup>10</sup> various 6-membered heterocycles based on **E**, which have been difficult to obtain and remain unknown, should be synthesized. Therefore, the establishment of a strategy for Type *endo-t* is an important challenge in heterocyclic chemistry.



**Scheme 2** (A) Four Types of Metalated Heterocycles from Oxymetalation of Alkyne **A** Including Carbonyl Moiety. (B) Comparison of Transition States of Type *Exo-t* with Type *Endo-t*.

Isocoumarins are an important class of oxygen-containing heterocycles that exhibit a wide range of pharmacological properties.<sup>11</sup> Thus, the development of their general synthetic method has attracted much attention. The reaction of Type *endo* would be a powerful tool for the synthesis of isocoumarins (Scheme 3A). In fact, reports have described the oxymetalation of 2-alkynylbenzoate **1** (R = alkyl, alkenyl, aryl) for Type *endo-i* and application to the synthesis of isocoumarins.<sup>6a,6b,6e</sup> Recently, Blum reported an excellent method for the construction of 4-borylated isocoumarins by oxyboration of the internal alkynes **1** in the Type *endo-i* reaction course (Scheme 3B).<sup>6e</sup> However, terminal alkyne **1** (R = H) gave only a 5-*exo* cyclization product according to the Markovnikov rule (blue path in Scheme 3C).<sup>6e</sup> This result prompted us to explore oxymetalation of the terminal alkynes **1** for Type *endo-t*. Oxymetalation of Type *endo-t* provides 3-unsubstituted and 4-substituted isocoumarins that are seldom investigated due to the lack of synthetic methods,<sup>12</sup> and limited substituents have been introduced at the 4-position despite well-known beneficial significant bioactivity characteristics such as antitumor,<sup>13</sup> antiangiogenic,<sup>14</sup> antifungal,<sup>15</sup> and antibiotic.<sup>16</sup>

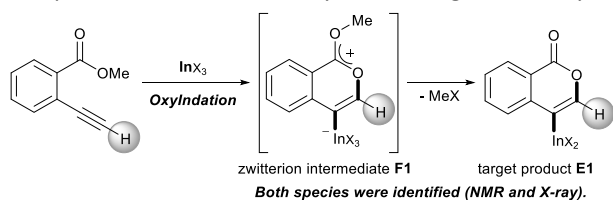


**Scheme 3** (A) Oxymetalation of 2-Alkynylbenzoate **1** Followed by Transformation for the Construction of Isocoumarins. (B) Previously Reported Oxyboration of Internal Alkynes to Generate 4-Borylated Isocoumarins. (C) Oxymetalation of Terminal Alkynes, Reported Oxyboration for 5-Membered Compounds (Blue Path), and Our Developed Oxymetalation for 6-Membered Compounds (Red Path).

Our group developed the indium or gallium salt-mediated carbometalation of simple terminal alkynes with silyl ketene acetals by utilizing their high  $\pi$  electron affinity and moderate Lewis acidity.<sup>17</sup> In this context, we investigated the Type *endo-t* reaction of 2-ethynylbenzoate using indium or gallium trihalides



for the synthesis of corresponding metalated isocoumarins. In this report, we successfully achieved a 6-*endo* selective oxy-metalation of terminal alkynes and fully characterized the target organometallic species **E1** via NMR study and X-ray crystallographic analysis. Furthermore, the intermediate **F1** was isolated, which revealed that oxy-metalation proceeds via the zwitterion intermediate **F1**, and elimination of the alkyl halide gives the target product **E1** (Scheme 4). While benzopyrylium species such as **F** are known as highly reactive intermediates in the proposed catalytic oxy-metalation cycle,<sup>10a,18</sup> the isolation of species **F** is a challenge issue.<sup>10e,10f,19</sup> To the best of our knowledge, **F1** is the first example of a fully characterized benzopyrylium intermediate **F**. In addition, we performed full disclosure of the mechanism by combining experimental data and theoretical calculation. These mechanistic investigations were consistent with the achievement of isolation of the zwitterion intermediate and demonstrated that its stability is a crucial point in this remarkable cyclization regioselectivity.



**Scheme 4** Oxyindation of Alkynes for Synthesis of Isocoumarin Framework via a Zwitterion Intermediate.

## Results and discussion

### Optimization of reaction conditions

First, we examined the effect of Lewis acids on oxy-metalation using methyl 2-ethynylbenzoate **1a** (Table 1). The reaction of **1a** with metal halides was carried out in toluene at 50 °C, and the reaction mixture was quenched with acetic acid. The reaction using InCl<sub>3</sub> afforded the target isocoumarin **2** via 6-*endo* cyclization, albeit in a low yield (entry 1). Gratifyingly, InBr<sub>3</sub> and InI<sub>3</sub> mediated oxy-metalation smoothly proceeded in 6-*endo* cyclization fashion to give **2** in high yields (entries 2 and 3). In these cases, the reaction mixture was quenched by deuterated acetic acid to afford **2** bearing deuterium at the 4-position. We did not observe an isocoumarin bearing deuterium at the 3-position which could be produced through the generation of indium acetylide<sup>20</sup> followed by Lewis acid mediated cycloaddition. The reaction using InI<sub>3</sub> showed a higher ratio of D/H than the case of InBr<sub>3</sub>. This result suggested the more efficient generation of the alkenylmetal intermediate **X** in the case of InI<sub>3</sub>. Gallium salts were also suitable for the 6-*endo* cyclization of **1a**, and GaI<sub>3</sub> gave a high yield (entries 4 and 5). On the other hand, typical Lewis acids such as AlCl<sub>3</sub>, AlI<sub>3</sub>, BBr<sub>3</sub> and TiCl<sub>4</sub> were ineffective (entries 6-9). Transition metal salts such as PdCl<sub>2</sub>, CuBr<sub>2</sub> and FeBr<sub>3</sub> provided no target product and resulted in a decomposition of **1a** (entries 10-12). Alkynophilic  $\pi$ -acids such as gold and silver salts were subjected into the present cyclization. It was found that AuCl<sub>3</sub>, AuCl, AgOTf and AuCl/AgOTf resulted in low yields (entries 13-16). A decrease in yield was observed at lower temperature (entry 17). The solvent

effect was examined on oxyindation using InI<sub>3</sub>. Dichloroethane as a solvent provided a good yield while chlorobenzene and hexane afforded only moderate yields (entries 18-20). The yields were appreciably decreased in CH<sub>3</sub>CN and THF (entries 21 and 22) probably because the coordination of these solvents to InI<sub>3</sub> decreased the Lewis acidity. Finally, InI<sub>3</sub> was the most effective Lewis acid, and, therefore, we chose entry 3 to represent the optimal conditions.

**Table 1** Effect of Lewis Acids on the Oxy-metalation of 2-Ethynylbenzoate **1a**<sup>a</sup>

Entry	MX <sub>n</sub>	Solvent	Yield of <b>2</b> (%) <sup>b</sup>
1	InCl <sub>3</sub>	toluene	13
2 <sup>c</sup>	InBr <sub>3</sub>	toluene	82 (77% D)
3 <sup>c</sup>	InI <sub>3</sub>	toluene	79 (91% D)
4	GaBr <sub>3</sub>	toluene	30
5	GaI <sub>3</sub>	toluene	77
6	AlCl <sub>3</sub>	toluene	0
7	AlI <sub>3</sub>	toluene	0
8	BBr <sub>3</sub>	toluene	0
9	TiCl <sub>4</sub>	toluene	0
10	PdCl <sub>2</sub>	toluene	0
11	CuBr <sub>2</sub>	toluene	0
12	FeBr <sub>3</sub>	toluene	0
13	AuCl <sub>3</sub>	toluene	7
14	AuCl	toluene	5
15	AgOTf	toluene	31
16	AuCl/AgOTf	toluene	18
17 <sup>d</sup>	InI <sub>3</sub>	toluene	61
18	InI <sub>3</sub>	ClCH <sub>2</sub> CH <sub>2</sub> Cl	78
19	InI <sub>3</sub>	ClC <sub>6</sub> H <sub>5</sub>	57
20	InI <sub>3</sub>	hexane	57
21	InI <sub>3</sub>	CH <sub>3</sub> CN	17
22	InI <sub>3</sub>	THF	0

<sup>a</sup> Reaction conditions: **1a** (0.5 mmol), Lewis acid MX<sub>n</sub> (0.5 mmol), solvent (1 mL), 50 °C, 24 h. <sup>b</sup> The yield of **2** was determined by <sup>1</sup>H NMR. <sup>c</sup> The reaction mixture was quenched by CH<sub>3</sub>CO<sub>2</sub>D (30 equiv, 5 min) and a subsequent addition of H<sub>2</sub>O (10 mL). <sup>d</sup> 35 °C

### Mechanistic Investigation

To gain insight into the reaction mechanism, we used <sup>1</sup>H NMR spectroscopy to monitor the oxyindation. When 2-alkynylbenzoate **1a** was mixed with InI<sub>3</sub> in CDCl<sub>3</sub> at -30 °C, no reaction occurred. At -5 °C, some amount of a new product was observed (See Fig. S1 and S2 in ESI<sup>†</sup>). At room temperature, a large amount of white precipitation was formed. This white solid was also obtained in the reaction of **1a** with InI<sub>3</sub> in toluene at room temperature (Eq. 1). X-ray crystallographic analysis revealed that the white solid was a 6-membered oxacycle



zwitterion **3** bearing a carbon-indium bond (Fig. 1). The bond lengths of two carbon-oxygen bonds (C1-O1 = 1.267 Å, C1-O2 = 1.298 Å) in the zwitterion **3** existed between a C=O double bond (1.203 Å) and the single bond (1.377 Å) of a typical isocoumarin derivative,<sup>21</sup> and, thus, the positive charge was delocalized in an ester moiety. The indium atom was coordinated with three iodines and showed a distorted tetrahedral structure with a formal negative charge. The formed zwitterionic alkenyl indium **3** was heated at 50 °C in toluene to give a neutral alkenylindium product **4a**, quantitatively by elimination of MeI (Eq. 2). Although a suitable single crystal of **4a** for X-ray analysis was not obtained, we successfully conducted X-ray diffraction analysis of nitro-substituted alkenylindium **4b** produced from the 2-ethynyl-5-nitrobenzoate **1b** (Eq. 3 and Fig. 2). The bond lengths of C1-O1 (1.211 Å) and C1-O2 (1.367 Å) were similar to those of reported isocoumarin framework.<sup>21</sup> The indium complex **4b** displayed trigonal bipyramidal coordination with two THF ligands in axial positions. These results indicated a two-step pathway including a fast cyclization and a slow elimination of MeI during the 6-*endo* oxyindination processing from **1** to **4**.

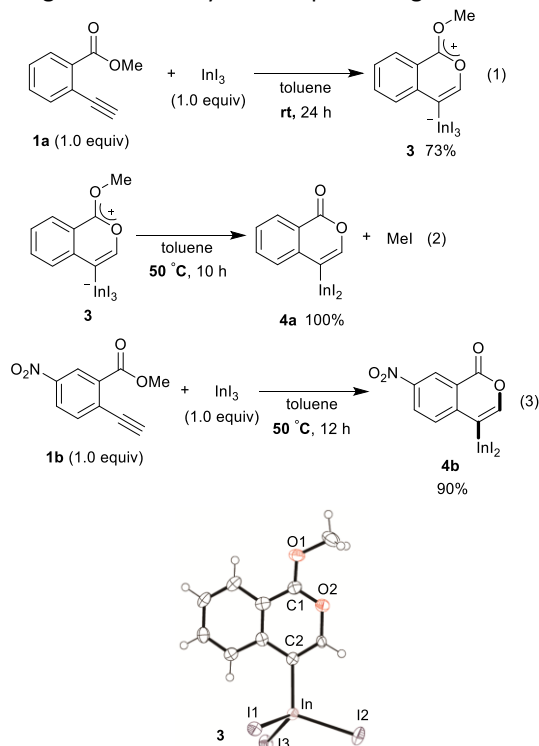


**Fig. 1** The X-ray crystallographic structure of zwitterion intermediate **3** with the thermal ellipsoids shown at 50% probability (CCDC 1579824). Selected bond lengths (Å): C1-O1 = 1.267(9), C1-O2 = 1.298(11), C2-In = 2.171(7), In-I1 = 2.7392(8), In-I2 = 2.7219(8), In-I3 = 2.6915(7).

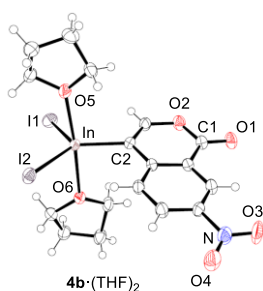
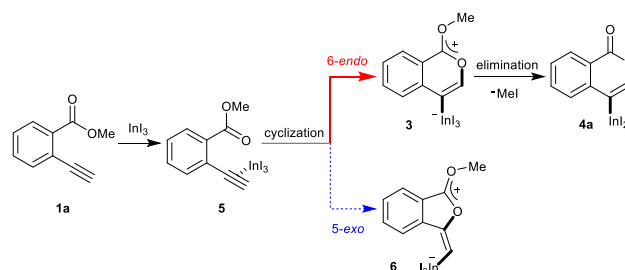


**Fig. 2** The X-ray crystallographic structure of isocoumarin including a carbon-indium bond at the 4-position, **4b**·(THF)<sub>2</sub>, with the thermal ellipsoids shown at 50%

probability (CCDC 1576342). Selected bond lengths (Å) and angles (deg): C1-O1 = 1.211(4), C1-O2 = 1.367(5), C2-In = 2.162(3), In-I1 = 2.7148(4), In-I2 = 2.7005(4), In-O5 = 2.318(3), In-O6 = 2.371(3), O5-In-O6 = 175.44(10), I1-In-C2 = 116.70(11), C2-In-I2 = 125.51(11), I2-In-I1 = 117.621(12).

### Theoretical Calculation for Oxyindination

A mechanism for the formation of the target isocoumarin **4a** using InI<sub>3</sub> is proposed in Scheme 5 wherein InI<sub>3</sub> is coordinated by the alkyne moiety in **5**, oxyindination proceeds via 6-*endo* cyclization to give the zwitterion intermediate **3**, and, finally, the elimination of MeI affords **4a**.



**Scheme 5** A Proposed Mechanism for Formation of the Isocoumarin **4a**.

Density functional theory (DFT) calculations were performed to more thoroughly consider the reaction mechanism. Calculation of the potential energy profile for 6-*endo* cyclization (red) shows in Fig. 3. We selected **1a** and In<sub>2</sub>I<sub>6</sub> as starting materials because InI<sub>3</sub> exists in a dimer fashion.<sup>22</sup> The coordination of two **1a** to In<sub>2</sub>I<sub>6</sub> dissociates the aggregation of InI<sub>3</sub> to give the complex **7**, in which InI<sub>3</sub> is chelated by the alkyne moiety and carbonyl group of **1a** (Fig. S3 in ESI<sup>†</sup> shows detail mechanism of generating the complex **7** from **1a** and In<sub>2</sub>I<sub>6</sub>). Dissociation of the carbonyl oxygen atom generates complex **5**, in which InI<sub>3</sub> directly activates the alkyne moiety. In this pathway, the anti-addition of InI<sub>3</sub> and the ester moiety into the alkyne moiety proceeds in a concerted mechanism to provide a stable 6-membered zwitterion intermediate **3**. Elimination of MeI proceeds in an intermolecular fashion, because the intramolecular elimination of MeI requires a very unstable intermediate (Fig. S4 in ESI<sup>†</sup> shows the potential energy profile for the intramolecular elimination of MeI). Two zwitterions aggregate in a head-to-tail fashion to give complex **8**, and then the elimination step starts from **8**. Intermolecular nucleophilic substitution of the methyl group by I<sup>-</sup> proceeds in an S<sub>N</sub>2-mechanism to give complex **10** and MeI, and then a subsequent elimination of MeI affords the target product **4a**.<sup>23</sup> A carbonyl group of **4a** coordinates to the indium atom of another **4a** to give the stable dimeric product **13**. The activation energy of the elimination step (**8** to TS2-6-*endo*, 28.7 kcal/mol) is much higher than that of the cyclization step (**7** to TS1-6-*endo*, 19.7 kcal/mol).<sup>24</sup> Therefore, the elimination of MeI is a rate-determining step. We also calculated the 5-*exo* cyclization pathway (blue) to investigate the regioselectivity. This process proceeds via concerted cyclization wherein the 5-membered zwitterion **6** is much more unstable than the 6-membered version **3**. Intermolecular elimination of MeI takes place in an S<sub>N</sub>2-manner (**9** to **11**). The energy level of the transition state (TS2-5-*exo*) shows the highest energy level, and it is higher even than the energy profile of the 6-*endo* cyclization process (red) due to the instability of the 5-membered zwitterion **6**.





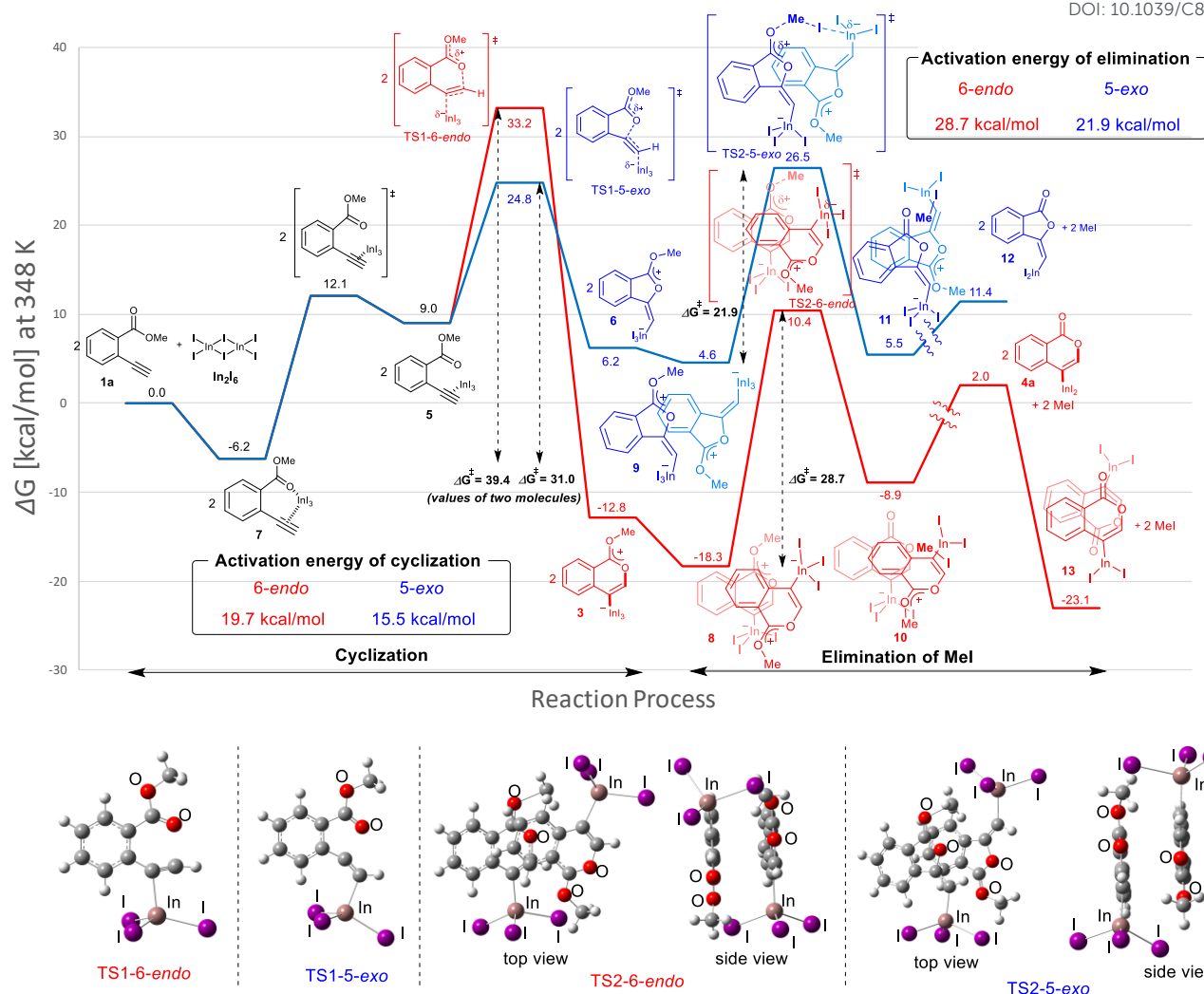


**Fig. 3** The energy profiles of 6-endo and 5-exo oxyindations and 3D molecular structures of transition states. DFT calculation was performed with wB97XD/6-31+G (d,p) for C, H, and O and using DGDZVP for In and I. Solvation effect was introduced using the IEFPCM model, and toluene was used as a solvent.

In order to clarify the unique 6-endo cyclization selectivity of oxyindation, the energy profiles of the two cyclization manners were compared. The activation energy of 5-exo cyclization is lower (7 to TS1-5-exo, 15.5 kcal/mol) than that of 6-endo cyclization (7 to TS1-6-endo, 19.7 kcal/mol). However, 5-exo cyclization is reversible because the activation energy for the elimination of MeI (9 to TS2-5-exo, 21.9 kcal/mol) is much higher than that of retro-cyclization (6 to TS1-5-exo, 9.3 kcal/mol) due to the instability of the zwitterion 6. On the other hand, during 6-endo cyclization, both activation energies of elimination (8 to TS2-6-endo, 28.7 kcal/mol) and retro-cyclization (3 to TS1-6-endo, 23.0 kcal/mol) are high because the 6-membered zwitterion intermediate 3 is thermodynamically stable. This result indicates that 6-endo cyclization is irreversible and the most thermodynamically stable form of intermediate 8 is exclusively generated to provide the target product 4a, which is consistent with the successful isolation of the zwitterion intermediate 3 (Fig. 1). Therefore, oxyindation proceeds under thermodynamic control to afford the stable 6-membered product 4a. We also calculated an energy profile of InCl<sub>3</sub>-

mediated oxyindation and found the same pathway with the case of InI<sub>3</sub> (See Fig. S5 in ESI†). The activation energy of elimination step in the cases of InCl<sub>3</sub> is higher than that of InI<sub>3</sub> because of low nucleophilicity of Cl<sup>-</sup>, and it caused much less reactivity of InCl<sub>3</sub> (entry 1, Table 1).

The remarkable regioselectivity of oxyindation is ascribed to the differences in stability between the 6-membered zwitterion 3 and the 5-membered 6. Zwitterion 3 is much more stable than 6, and this difference in stability originates from the aromaticity of these compounds, although ring strain is also a consideration. To verify this possibility, the aromaticity of zwitterions was evaluated via NICS(1)<sup>25</sup> (Fig. 4), and the 6-membered compound 3 showed a higher level of aromaticity than that of 6.



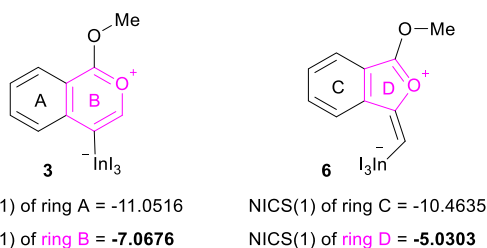
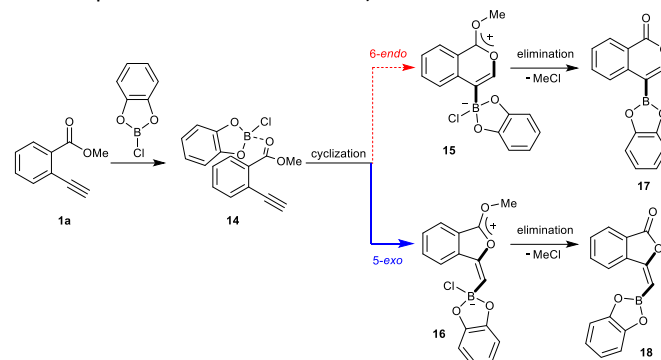


**Fig. 4** NICS(1) values of 6-membered zwitterion **3** and 5-membered zwitterion **6**. The aromaticity was calculated using B3LYP/6-31G (d,p) for C, H, and O and using DGDZVP for In and I for their optimized structures.

### Theoretical Calculation for Oxyboration

Blum and co-workers reported that oxyboration of **1a** using *B*-chlorocatecholborane (ClBcat) gave a 5-membered product<sup>6e</sup> rather than the 6-membered version (Scheme 6). ClBcat is coordinated by the carbonyl moiety of **1a**. Then, oxyboration proceeds via 5-*exo* cyclization to give the zwitterion intermediate **16**, and the elimination of MeCl gives the target product **18**. We also performed DFT calculation of oxyboration to investigate the striking change in the regioselectivity between oxyboration and oxyindation. First, the calculation of oxyboration was performed for a similar oxyindation mechanism via concerted cyclization and S<sub>N</sub>2-type elimination of MeCl from aggregated zwitterion intermediates (see Fig. S6 in ESI<sup>†</sup>). We considered another possibility for the elimination step, because recent theoretical investigation of ClBcat-mediated heterocyclization has shown other mechanisms,<sup>26</sup> whereby the Me group is attacked either by dissociated chloride<sup>26a</sup> or by [Cl<sub>2</sub>Bcat]<sup>-</sup>.<sup>26b</sup> Thus, we considered these additional two plausible elimination steps assisted either by free Cl<sup>-</sup> or [Cl<sub>2</sub>Bcat]<sup>-</sup> (See Fig. S7 in ESI<sup>†</sup> and Fig. 5 and 6). The

result of comparison between these three pathways showed that the most probable path was the use of [Cl<sub>2</sub>Bcat]<sup>-</sup> (Details of the comparison are shown in ESI<sup>†</sup>).



**Scheme 6 A** Proposed Mechanism for Oxyboration.

The total reaction profile of oxyboration is described in Fig. 5 and 6. In that profile, 5-*exo* cyclization from **1a** and 2ClBcat to **16** has an activation energy (27.9 kcal/mol) that is lower than that of 6-*endo* cyclization (**1a** and 2ClBcat to **15**, 34.4 kcal/mol). The chloride moiety of zwitterion **16** coordinates to another ClBcat to provide complex **19**. The chloride transfer process (**19** to **20**) has a low energy barrier (5.8 kcal/mol), and [Cl<sub>2</sub>Bcat]<sup>-</sup> is generated rapidly. Cl in [Cl<sub>2</sub>Bcat]<sup>-</sup> approaches the methyl group in the ester moiety (**20**→**21**→**22**), and an elimination of MeCl (**22** to **23**) in the S<sub>N</sub>2-mechanism occurs to give 5-membered product **18**. The activation energy of the elimination of MeCl (**22** to TS3-5-*exo*) is 20.7 kcal/mol, which allows the elimination of MeCl to proceed smoothly to give the final product **18**. The fast elimination step allows oxyboration to proceed under kinetic control to accomplish the 5-*exo* selective cyclization.

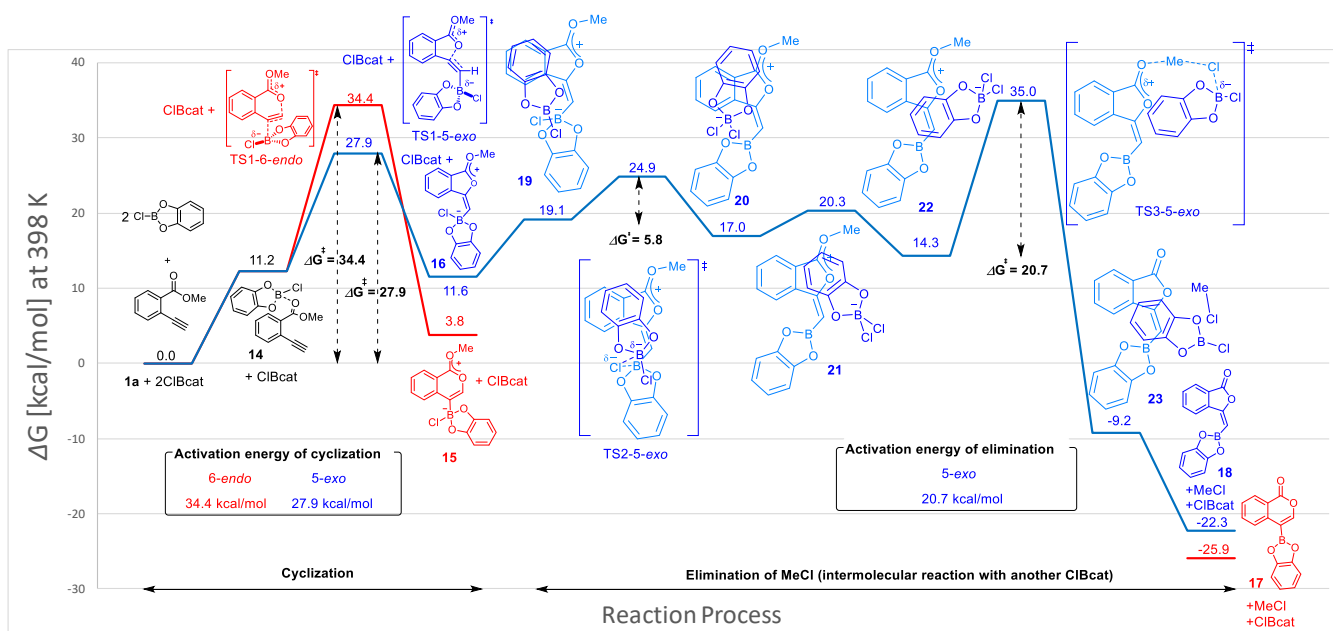


**Fig. 5** The energy profiles of 5-*exo* and 6-*endo* oxyborations. DFT calculation was performed by wb97XD/6-31+G (d,p) for C, H, O, B, and Cl. Solvation effect was introduced using the IEFPCM model, and toluene was used as a solvent.



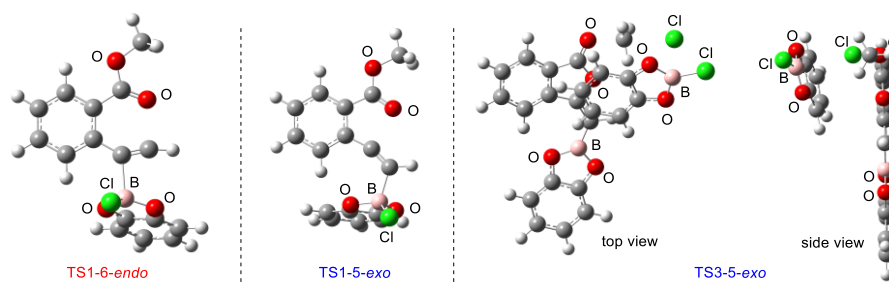


Fig. 6 3D molecular structures of transition states in oxyborations.

### Comparing the Transition State of the Cyclization Step in Oxyindation with That in Oxyboration Based on an Electrostatic Potential Map

The significant difference between oxyindation and oxyboration was investigated because each showed a characteristic energy profile, particularly for the cyclization step. The energy barrier of cyclization in oxyindation (6-*endo*: 19.7 kcal/mol, 5-*exo*: 15.5 kcal/mol) is much lower than that of oxyboration (6-*endo*: 34.4 kcal/mol, 5-*exo*: 27.9 kcal/mol). Therefore, the electrostatic potential maps for the transition states of cyclization (TS1-6-*endo* and TS1-5-*exo*) were calculated (Fig. 7). The value of  $V_{\min}$ , which represents the most negative surface electrostatic potential, was investigated to evaluate the degree of localization for a negative charge.<sup>27</sup> The  $V_{\min}$  of the organoindium species (left, in Fig. 7) was less negative than that of boron (right, in Fig. 7), which showed that the negative charge was delocalized in the transition state of oxyindation compared with oxyboration. The value of  $V_{\max}$ , which is the most positive surface electrostatic potential, was also calculated and was less affected by the differences in the metals (see Table S2 in ESI†). The polarizability of the indium, boron and heteroatoms binding to a metal explained these results. Indium and iodine atoms have large polarizability ( $\alpha_{\text{In}} = 69$  a.u.,  $\alpha_{\text{I}} = 35.1$  a.u.),<sup>28</sup> and the increasing negative charge in the TS1 of oxyindation was efficiently delocalized to stabilize the zwitterionic TS1-6-*endo*.<sup>29</sup> On the other hand, boron, chlorine and oxygen atoms have smaller polarizability ( $\alpha_{\text{B}} = 20.5$  a.u.,  $\alpha_{\text{Cl}} = 14.7$  a.u.,  $\alpha_{\text{O}} = 6.04$  a.u.)<sup>28</sup> than indium and iodine atoms, so that TS1-5-*exo* becomes unstable due to the localization of a negative charge. The difference in the fundamental features

between indium and boron atoms imparts a significant amount of influence to the regioselectivity of oxymetalation.

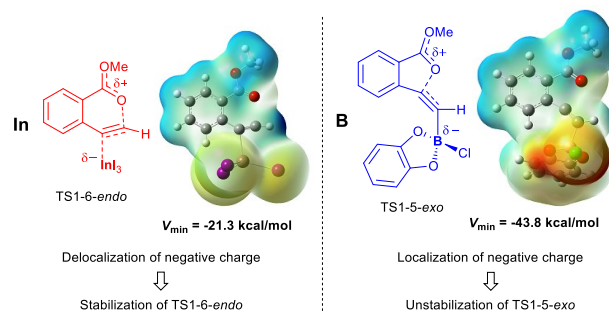


Fig. 7 Electrostatic potential maps were calculated on the 0.001 au isosurface of electron density for optimized structures of the transition states of oxyindation (left) and oxyboration (right). The potential is depicted by a color gradient from the most negative (red) to the most positive (blue) value (kcal/mol).  $V_{\min}$  represents the most negative surface electrostatic potential.

### Summary of DFT Calculation

In oxyindation (Fig. 8A), the activation energy of 5-*exo* cyclization is much lower than that required for the elimination of MeI to lead reversible 5-*exo* cyclization. Therefore, the thermodynamically stable 6-membered zwitterion **3** was selectively produced to accomplish the remarkable 6-*endo* selectivity. The elimination step from **3** is a rate-determining step that provides the target metalated isocoumarin **4a**. On the other hand, the energy barrier for cyclization in oxyboration (Fig. 8B) is higher than that for the elimination of MeCl and the cyclization step is a rate-determining step, which leads to irreversible 5-*exo* cyclization to afford the 5-membered product **18** under kinetic control. Therefore, activation energies of cyclization as well as elimination are important factors to determine the regioselectivity in cyclization.

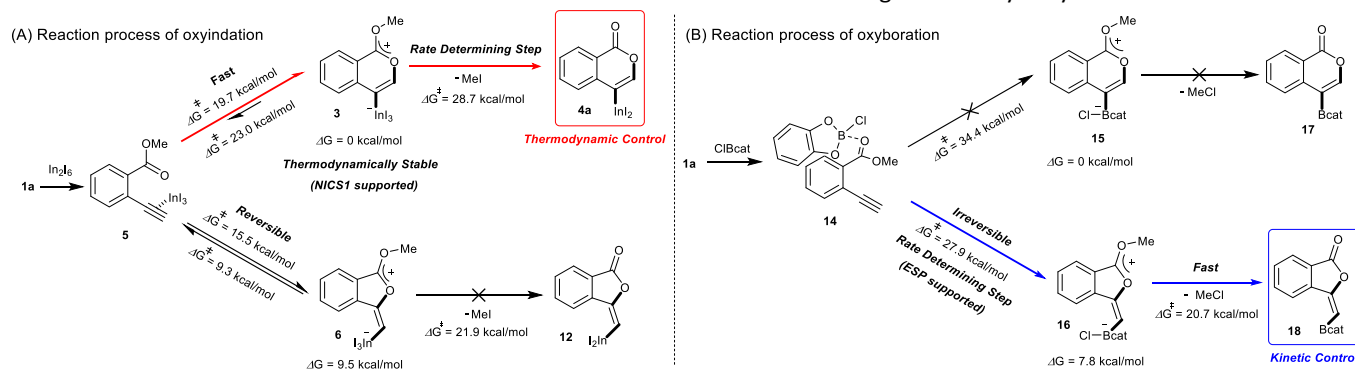


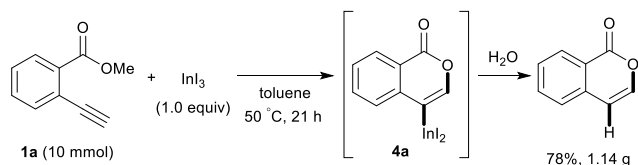
Fig. 8 The summarized results of DFT calculation.





## Application to the Synthesis of Isocoumarin Derivatives

Our developed oxyindation was applied to the synthesis of isocoumarin derivatives. First, the gram-scale synthesis of an organoindium species was carried out. Methyl ester **1a** (10 mmol) reacted with  $\text{InI}_3$  to give organoindium **4a**, and 1.14 g of isocoumarin was isolated by the addition of  $\text{H}_2\text{O}$  (Scheme 7).



**Scheme 7** Gram-Scale Synthesis of Isocoumarin Including a Carbon-Indium Bond.

Next, the oxidation of produced alkenylindium compounds was performed (Table 2). An oxyindation of **1a** using  $\text{InI}_3$  was carried out, and the organoindium **4a** was oxidized by  $\text{PhI}(\text{OAc})_2$  in a one-pot procedure to give 4-iodoisocoumarin **24a** (entry 1). Subjecting  $\text{InBr}_3$  to the oxidation reaction provided 4-bromoisocoumarin **25a** in a high yield (entry 2). Therefore, various types of 2-alkynylbenzoates were surveyed in the sequential oxyindation/halogenation process to give 4-halogenated isocoumarins. Substrates with electron withdrawing groups such as nitro and carbonyl groups gave the target products **24b** and **24c** in high yields (entries 3 and 4). The structure of **24b** was characterized by X-ray crystallographic analysis (See Fig. S11 in ESI<sup>†</sup>). Substrates with methyl or aryl groups efficiently afforded the target isocoumarins **24d** and **24e** (entries 5 and 6). Also, 2-alkynylbenzoates, including halogen moieties (Br, Cl and F), were suitable for this reaction system to give the isocoumarins **25f-24h** in moderate yields (entries 7-9). The synthesis of isocoumarins from internal alkynes was also investigated. Optimization of the reaction conditions showed that gallium salts were more suitable than indium salts for the oxyindation of an internal alkyne (See Table S3 in ESI<sup>†</sup>). Therefore, gallium salts were employed in the reactions of internal alkynes **1i**, **1j** and **1k** to provide the 3,4-disubstituted isocoumarins **24i**, **24j** and **25k** (entries 10-12).

One-pot syntheses of 4-substituted isocoumarins were performed via oxyindation followed by a palladium-catalyzed cross-coupling reaction (Table 3).<sup>30</sup> After the oxyindation of **1a** using  $\text{InBr}_3$ , the addition of a palladium catalyst, lithium chloride, organic halides **27**, and an additional solvent to the resultant toluene solution afforded the coupling product **28**. Iodobenzene **27a** and the aryl iodides bearing electron donating group **27b** or electron withdrawing group **27c** were applicable to give the 4-arylisocoumarins **28aa-28ac** in high yields (entry 1). Palladium-catalyzed cross coupling with acid chlorides also proceeded efficiently. Reactions using the benzoyl chloride derivatives **27d** and **27e**, as well as the alkanoyl chloride **27f**, afforded the isocoumarins **28ad-28af** with ketone moieties in good yields (entries 2 and 3). The structure of **28ae** was characterized by X-ray crystallographic analysis (See Fig. S12 in ESI<sup>†</sup>). In this reaction system, alkyl halides such as the benzyl bromide **27g** and the allyl bromide **27h** were also suitable to give the 4-alkylisocoumarins **28ag** and **28ah**, respectively (entries 4 and 5). Various types of 4-substituted isocoumarins

were obtained from an isocoumarin that included a carbon-indium bond by utilizing palladium-catalyzed cross-coupling

**Table 2** Sequential Oxyindation/Halogenation of Various Types of 2-Alkynylbenzoate **1**<sup>a</sup>

Entry	<b>1</b>	$\text{MX}_3$	Target	Yield (%) <sup>b</sup>
1		$\text{InI}_3$		64
2		$\text{InBr}_3$		73
3		$\text{InI}_3$		61
4		$\text{InI}_3$		70
5		$\text{InI}_3$		54
6		$\text{InI}_3$		54
7		$\text{InBr}_3$		47
8		$\text{InI}_3$		67
9		$\text{InI}_3$		61
10		$\text{GaI}_3$		60
11		$\text{GaI}_3$		56
12		$\text{GaBr}_3$		60

<sup>a</sup> First step: **1** (0.5 mmol),  $\text{MX}_3$  (0.5 mmol), toluene (1 mL), 50 °C, 24 h. Second step:  $\text{PhI}(\text{OAc})_2$  (1.0 mmol),  $\text{Et}_2\text{O}$  (1 mL), rt, 12 h. <sup>b</sup> Isolated yields.



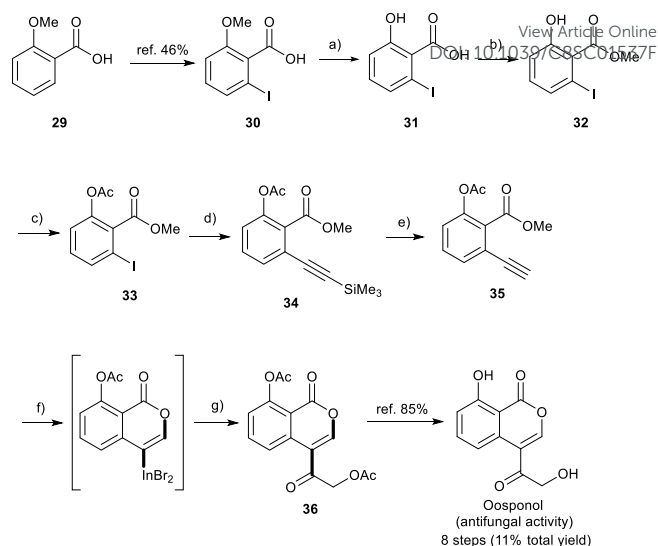
**Table 3** One-Pot Formation of 4-Substituted Isocoumarins by Palladium-Catalyzed Cross Coupling of Organoindium Species **26** with Organic Halides **27**<sup>a</sup>

Entry		27	Target	Yield (%) <sup>b</sup>
1		<b>27a</b> (R = H) <b>27b</b> (R = OMe) <b>27c</b> (R = CN)	<b>28aa</b> (R = H) <b>28ab</b> (R = OMe) <b>28ac</b> (R = CN)	<b>28aa</b> : 81 <b>28ab</b> : 71 <b>28ac</b> : 72
2		<b>27d</b> (R = H) <b>27e</b> (R = Cl)	<b>28ad</b> (R = H) <b>28ae</b> (R = Cl)	<b>28ad</b> : 82 <b>28ae</b> : 64
3 <sup>c</sup>		<b>27f</b>	<b>28af</b>	61
4 <sup>d</sup>		<b>27g</b>	<b>28ag</b>	51
5 <sup>d</sup>		<b>27h</b>	<b>28ah</b>	45 <sup>e</sup>

<sup>a</sup> Basic reaction conditions of the first step: **1a** (0.5 mmol), InBr<sub>3</sub> (0.5 mmol), toluene (1 mL), 50 °C, 24 h. Second step: Pd<sub>2</sub>(dba)<sub>3</sub> (0.025 mmol), LiCl (1.0 mmol), **27** (1.0 mmol), NMP (2.5 mL), 50 °C, 24 h. <sup>b</sup> Isolated yields. <sup>c</sup> HMPA (2.5 mL), rt, 24 h. <sup>d</sup> HMPA (2.5 mL), 50 °C, 24 h. <sup>e</sup> E/Z = 90:10.

### Formal Total Synthesis of Oosponol

Finally, a formal total synthesis of oosponol, which exhibits strong antifungal activity,<sup>15</sup> was conducted (Scheme 8). Firstly, iodination of commercially available compound **29** proceeded via a method found in the literature.<sup>31</sup> During the initial investigation, **30** was transformed into methyl 2-ethynyl-6-methoxybenzoate, and then we attempted the synthesis of the precursor of oosponol via oxyindation and cross-coupling, but the reaction returned a complicated mixture (See Scheme S1 in ESI<sup>†</sup>). Therefore, in another synthetic route, the OMe group of **29** was converted to an OAc group with less ability to donate electrons. The OMe moiety of **30** was completely deprotected by BBr<sub>3</sub>. Acid-catalyzed esterification and acetylation of the phenol moiety gave methyl 6-iodoacetylsalicylate **33** in a high yield. Sonogashira coupling followed by the removal of a silyl moiety afforded the desired 2-alkynylbenzoate derivative **35**. Oxymetalation of **35** using InBr<sub>3</sub> and sequential palladium-catalyzed cross coupling with acid chloride **27i** produced the key intermediate **36**, and the hydrolyzation of **36** yielded oosponol.<sup>16b</sup> Our method used a readily available starting material and gave a higher yield than previous works.<sup>16b,32</sup>



**Scheme 8** Formal Total Synthesis of Oosponol. Reagents and reaction conditions: a) BBr<sub>3</sub> (1 M in CH<sub>2</sub>Cl<sub>2</sub>, 2.0 equiv), CH<sub>2</sub>Cl<sub>2</sub>, RT, 20 h, 100%. b) H<sub>2</sub>SO<sub>4</sub> (20 mol %), MeOH, Reflux, 20 h, 87%. c) AcCl (1.04 equiv), Pyridine (1.04 equiv), Acetone, RT, 14 h, 97%. d) Ethynyltrimethylsilane (1.1 equiv), PdCl<sub>2</sub>(PPh<sub>3</sub>)<sub>2</sub> (2.0 mol %), CuI (20 mol %), NEt<sub>3</sub>, RT, 17 h, 100%. e) 1M KF aq. (1.65 equiv), DMF, RT, 0.5 h, 76%. f) InBr<sub>3</sub> (1.0 equiv), Toluene, 50 °C, 24 h. g) Pd<sub>2</sub>(dba)<sub>3</sub> (5.0 mol %), LiCl (2.0 equiv), 2-(acetoxy)acetyl chloride **27i** (2.0 equiv), HMPA, RT, 9 h, 44%.

### Conclusions

We achieved the synthesis of isocoumarins bearing a metal-carbon bond at the 4-position via 6-*endo* selective oxymetalation of 2-alkynylbenzoate **1** (Type *endo-t*). Indium and gallium salts showed high activity for the oxymetalation of 2-ethynylbenzoate **1a**. Both the metalated isocoumarin **4b** and the zwitterion intermediate **3** were identified by X-ray crystallographic analysis. This is the first example of the isolation of the product **E** and the benzopyrylium intermediate **F** proposed in the mechanism of oxymetalation (Scheme 2A). The elimination of MeI from zwitterion **3** occurred under heating conditions to give the target product **4a**, which means the rate-determining step was the elimination step. DFT calculation suggested that thermodynamic control led to 6-*endo* selective oxyindation, while kinetic control led to 5-*exo* selective oxyboration. The 6-membered product proved much more stable than the 5-membered product due to a difference in the degree of aromatic stability. The investigation of electrostatic potential of the transition state in the cyclization pathway suggested that a delocalization of negative charge by large atomic radii of In and I atoms stabilizes the zwitterionic transition state. In contrast, small atomic radii of B, Cl, and O atoms causes a localization of negative charge to destabilize the corresponding transition state. The difference in stability between the 6- and 5-membered zwitterions and the elemental character of InI<sub>3</sub> both played important roles in the unique regioselectivity of oxymetalation and in the facile preparation of the **E** species.

These isocoumarins bearing a carbon-metal bond at the 4-position were applied to organic synthesis. Oxymetalation provided isocoumarins on a gram scale. The oxidation of organoindium or gallium species yielded various types of 4-halogenated isocoumarins. Palladium-catalyzed cross coupling



with aryl iodide, acid chloride, and alkyl bromide gave a wide range of 4-substituted isocoumarins in a one-pot reaction. Therefore, the unprecedented regioselectivity of the present oxymetalation contributed to the synthesis of new types of isocoumarins. We accomplished a formal total synthesis of oosponol to demonstrate the utility of our reaction system.

## Conflicts of interest

There are no conflicts to declare.

## Acknowledgements

This work was supported by JSPS KAKENHI Grant Numbers JP15H05848 in Middle Molecular Strategy and JP16K05719. Y.N. acknowledges support from the Frontier Research Base for Global Young Researchers, Osaka University, of the MEXT program and from Mitsui Chemicals Award in Synthetic Organic Chemistry. We thank Prof. Dr. S. Blum (Department of Chemistry, University of California, Irvine) for helpful suggestions. We would like to thank Prof. Dr. S. Akai (Graduate School of Pharmaceutical Science, Osaka University, Japan) for suggestions about total synthesis of oosponol. Thanks are due to the Analytical Instrumentation Facility, Graduate School of Engineering, Osaka University, for assistance in obtaining the MS spectra.

## Notes and references

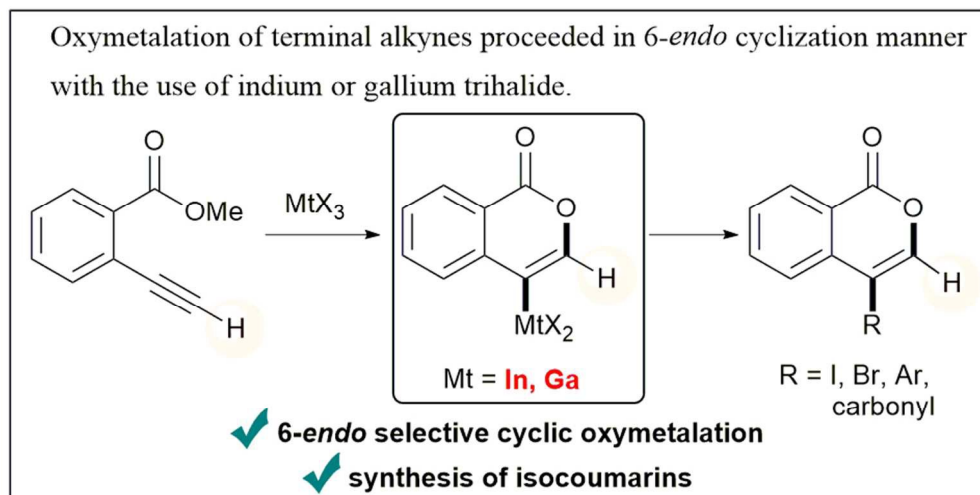
- (a) D. B. Kitchen, H. Decornez, J. R. Furr and J. Bajorath, *Nat. Rev. Drug Discovery*, 2004, **3**, 935-949; (b) R. E. Ziegert, J. Tor ng, K. Knepper and S. Br se, *J. Comb. Chem.*, 2005, **7**, 147-169; (c) R. A. Ward and J. G. Kettle, *J. Med. Chem.*, 2011, **54**, 4670-4677; (d) P. S. Mariano, *Tetrahedron*, 1983, **39**, 3879-3983; (e) N. A. Romero and D. A. Nicewicz, *Chem. Rev.*, 2016, **116**, 10075-10166; (f) B. H. Lipshutz, *Chem. Rev.*, 1986, **86**, 795-819; (g) A. R. Katritzky, *Chem. Rev.*, 1989, **89**, 827-861; (h) Y.-G. Zhou, *Acc. Chem. Res.*, 2007, **40**, 1357-1366.
- (a) R. Dorel and A. M. Echavarren, *Chem. Rev.*, 2015, **115**, 9028-9072; (b) N. T. Patil and Y. Yamamoto, *Chem. Rev.*, 2008, **108**, 3395-3442; (c) F. Alonso, I. P. Beletskaya and M. Yus, *Chem. Rev.*, 2004, **104**, 3079-3159; (d) A. Deiters and S. F. Martin, *Chem. Rev.*, 2004, **104**, 2199-2238; (e) V. Nair, C. Rajesh, A. U. Vinod, S. Bindu, A. R. Sreekanth, J. S. Mathen and L. Balagopal, *Acc. Chem. Res.*, 2003, **36**, 899-907.
- For selective examples: (a) J. Liu, X. Xie and Y. Liu, *Chem. Commun.*, 2013, **49**, 11794-11796; (b) Y.-J. Feng, F.-Y. Tsai, S.-L. Huang, Y.-H. Liu and Y.-C. Lin, *Eur. J. Inorg. Chem.*, 2014, 5406-5414; (c) S. S. Racharlawar, D. Shankar, M. V. Karkhelikar, B. Sridhar and P. R. Likhar, *J. Organomet. Chem.*, 2014, **757**, 14-20; (d) J. J. Hirner, D. J. Faizi and S. A. Blum, *J. Am. Chem. Soc.*, 2014, **136**, 4740-4745; (e) D. Shankar, K. Jaipal, B. Sridhar, R. N. Chary, S. Prabhakar, L. Giribabu and P. R. Likhar, *RSC Adv.*, 2015, **5**, 20295-20301; (f) E. Chong and S. A. Blum, *J. Am. Chem. Soc.*, 2015, **137**, 10144-10147; (g) K. N. Tu, J. J. Hirner and S. A. Blum, *Org. Lett.*, 2016, **18**, 480-483; (h) D. J. Faizi, N. A. Nava, M. Al-Amin and S. A. Blum, *Org. Synth.*, 2016, **93**, 228-244; (i) D. J. Faizi, A. J. Davis, F. B. Meany and S. A. Blum, *Angew. Chem. Int. Ed.*, 2016, **55**, 14286-14290; (j) A. J. Warner, A. Churn, J. S. McGough and M. J. Ingleson, *Angew. Chem. Int. Ed.*, 2017, **56**, 354-358; (k) N. Chaisan, W. Kaewsri, C. Thongsornkleeb, J. Tummatorn and S. Ruchirawat, *Tetrahedron Lett.*, 2018, **59**, 675-680. DOI: 10.1039/C8SC01537F
- (a) Y. Kato, K. Miki, F. Nishino, K. Ohe and S. Uemura, *Org. Lett.*, 2003, **5**, 2619-2621; (b) C. P. Casey, N. A. Strotman and I. A. Guzei, *Organometallics*, 2004, **23**, 4121-4130; (c) R. Vicente, J. Gonz lez, L. Riesgo, J. Gonz lez and L. A. L pez, *Angew. Chem. Int. Ed.*, 2012, **51**, 8063-8067; (d) T. Murata, M. Murai, Y. Ikeda, K. Miki and K. Ohe, *Org. Lett.*, 2012, **14**, 2296-2299; (e) Y. Xia, S. Qu, Q. Xiao, Z.-X. Wang, P. Qu, L. Chen, Z. Liu, L. Tian, Z. Huang, Y. Zhang and J. Wang, *J. Am. Chem. Soc.*, 2013, **135**, 13502-13511; (f) J.-M. Yang, Z.-Q. Li, M.-L. Li, Q. He, S.-F. Zhu and Q.-L. Zhou, *J. Am. Chem. Soc.*, 2017, **139**, 3784-3789.
- (a) K. Miki, T. Yokoi, F. Nishino, K. Ohe and S. Uemura, *J. Organomet. Chem.*, 2002, **645**, 228-234; (b) K. Miki, T. Yokoi, F. Nishino, Y. Kato, Y. Washitake, K. Ohe and S. Uemura, *J. Org. Chem.*, 2004, **69**, 1557-1564; (c) K. Okamoto, M. Watanabe, A. Mashida, K. Miki and K. Ohe, *Synlett*, 2013, **24**, 1541-1544.
- (a) R. C. Larock and L. W. Harrison, *J. Am. Chem. Soc.*, 1984, **106**, 4218-4227; (b) A. Nagarajan and T. R. Balasubramanian, *Indian J. Chem. B*, 1987, **26B**, 917-919; (c) Y. Zhu and B. Yu, *Angew. Chem. Int. Ed.*, 2011, **50**, 8329-8332; (d) Y. Tang, J. Li, Y. Zhu, Y. Li and B. Yu, *J. Am. Chem. Soc.*, 2013, **135**, 18396-18405; (e) D. J. Faizi, A. Issaian, A. J. Davis and S. A. Blum, *J. Am. Chem. Soc.*, 2016, **138**, 2126-2129; (f) B. Akkachairin, J. Tummatorn, N. Supantanapong, P. Nimnual, C. Thongsornkleeb and S. Ruchirawat, *J. Org. Chem.*, 2017, **82**, 3727-3740.
- The metal species **E** was proposed as intermediate for oxymetalation/protonation sequential reactions, and these cyclic reactions showed low regioselectivity to afford mixture of 5- and 6-membered rings. (a) E. Marchal, P. Uriac, B. Legouin, L. Toupet and P. v. d. Weghe, *Tetrahedron*, 2007, **63**, 9979-9990; (b) B. Y.-W. Man, A. Knuhtsen, M. J. Page and B. A. Messerle, *Polyhedron*, 2013, **61**, 248-252.
- (a) I. V. Alabugin, K. Gilmore and M. Manoharan, *J. Am. Chem. Soc.*, 2011, **133**, 12608-12623. (b) K. Gilmore, R. K. Mohamed and I. V. Alabugin, *WIREs: Comput. Mol. Sci.*, 2016, **6**, 487-514.
- (a) I. V. Alabugin and K. Gilmore, *Chem. Commun.*, 2013, **49**, 11246-11250. (b) P. W. Peterson, R. K. Mohamed and I. V. Alabugin, *Eur. J. Org. Chem.*, 2013, 2505-2527. (c) T. Yao and R. C. Larock, *J. Org. Chem.*, 2003, **68**, 5936-5942.
- Although some groups reported 6-endo cyclic oxymetalation using terminal alkynes, the formed 6-membered pyrylium intermediate **F** was trapped by a nucleophile to give **E** but heterocyclic compounds or naphthalene derivatives, and **F** has not been isolated. (a) N. Iwasawa, M. Shido and H. Kusama, *J. Am. Chem. Soc.*, 2001, **123**, 5814-5815; (b) N. Asao, T. Nogami, K. Takahashi and Y. Yamamoto, *J. Am. Chem. Soc.*, 2002, **124**, 764-765; (c) H. Kusama, H. Funami, J. Takaya and N. Iwasawa, *Org. Lett.*, 2004, **6**, 605-608; (d) N. T. Patil and Y. Yamamoto, *J. Org. Chem.*, 2004, **69**, 5139-5142; (e) H. Kusama, H. Funami, M. Shido, Y. Hara, J. Takaya and N. Iwasawa, *J. Am. Chem. Soc.*, 2005, **127**, 2709-2716; (f) H. Kusama, H. Funami and N. Iwasawa, *Synthesis*, 2007, **13**, 2014-2024; (g) R. Yanada, K. Hashimoto, R. Tokizane, Y. Miwa, H. Minami, K. Yanada, M. Ishikura and T. Takemoto, *J. Org. Chem.*, 2008, **73**, 5135-5138; (h) X.-L. Fang, R.-Y. Tang, X.-G. Zhang, P. Zhong, C.-L. Deng and J.-H. Li, *J. Organomet. Chem.*, 2011, **696**, 352-356; (i) S. Zhu, Z. Zhang, X. Huang, H. Jiang and Z. Guo, *Chem. Eur. J.*, 2013, **19**, 4695-4700; (j) G. Mariaule, G. Newsome, R. Y. Toullec, P. Belmont and V. Michelet, *Org. Lett.*, 2014, **16**, 4570-4573; (k) J.-F. Cui, H.-M. Ko, K.-P. Shing, J.-R. Deng, N. C.-H. Lai and M.-K. Wong, *Angew. Chem. Int. Ed.*, 2017, **56**, 3074-3079.
- (a) R. D. Barry, *Chem. Rev.*, 1964, **64**, 229-260; (b) R. A. Hill in *Progress in the Chemistry of Organic Natural Products*, ed. W. Herz, Vol. 49, pp 1-78. (c) I.-U. Rahman, M. Arfan and G. A. Khan, *J. Chem. Soc. Pak.*, 1998, **20**, 76-87; (d) V. Rukachaisirikul, A. Rodglin, Y. Sukpondma, S. Phongpaichit, J. Buatong and J.



- Sakayaroj, *J. Nat. Prod.*, 2012, **75**, 853-858; (e) M. E. Riveiro, A. Moglioni, R. Vazquez, N. Gomez, G. Facorro, L. Piehl, E. R. De Celis, C. Shayo and C. Davio, *Bioorg. Med. Chem.*, 2008, **16**, 2665-2675; (f) L. M. Bedoya, E. Del Olmo, R. Sancho, B. Barboza, M. Beltrán, A. E. García-Cadenas, S. Sánchez-Palomino, J. L. López-Pérez, E. Muñoz, A. S. Feliciano and J. Alcamí, *Bioorg. Med. Chem. Lett.*, 2006, **16**, 4075-4079; (g) N. Agata, H. Nogi, M. Milhollen, S. Kharbanda and D. Kufe, *Cancer Res.*, 2004, **64**, 8512-8516; (h) T. Nakashima, S. Hirano, N. Agata, H. Kumagai, K. Isshiki, T. Yoshioka, M. Ishizuka, K. Maeda and T. Takeuchi, *J. Antibiot.*, 1999, **52**, 426-428; (i) M. Yoshikawa, E. Harada, Y. Noritoh, K. Inoue, H. Matsuda, H. Shimoda, J. Yamahara and N. Murakami, *Chem. Pharm. Bull.*, 1994, **42**, 2225-2230; (j) T. Furuta, Y. Fukuyama and Y. Asakawa, *Phytochemistry*, 1986, **25**, 517-520.
- 12 (a) N. Panda, P. Mishra and I. Mattan, *J. Org. Chem.*, 2016, **81**, 1047-1056; (b) K. Kobayashi, W. Miyatani and M. Kuroda, *Helv. Chim. Acta.*, 2013, **96**, 2173-2178; (c) M. Lessi, T. Masini, L. Nucara, F. Bellina and R. Rossi, *Adv. Synth. Catal.*, 2011, **353**, 501-507; (d) M. P. Pavan, M. Chakravarty and K. C. K. Swamy, *Eur. J. Org. Chem.*, 2009, 5927-5940; (e) Z. He and A. K. Yudin, *Org. Lett.*, 2006, **8**, 5829-5832; (f) M. Chakravarty and K. C. K. Swamy, *J. Org. Chem.*, 2006, **71**, 9128-9138; (g) S. Kim, G.-J. Fan, J. Lee, J. J. Lee and D. Kim, *J. Org. Chem.*, 2002, **67**, 3127-3130; (h) B. A. Kowalczyk, *Synthesis*, 2000, **8**, 1113-1116; (i) P. Babin and J. Dunoguès, *Tetrahedron Lett.*, 1984, **25**, 4389-4392; (j) K. Beutement and J. M. Clough, *Tetrahedron Lett.*, 1984, **25**, 3025-3028; (k) O. S. Wolfbeis, *Liebigs Ann. Chem.*, 1981, 819-827.
- 13 M. Kimura, I. Waki and M. Kokubo, *Jpn. J. Pharmacol.*, 1978, **28**, 693-697.
- 14 J. H. Lee, Y. J. Park, H. S. Kim, Y. S. Hong, K.-W. Kim and J. J. Lee, *J. Antibiot.*, 2001, **54**, 463-466.
- 15 (a) J. Sonnenbichler and T. Kovács, *Eur. J. Biochem.*, 1997, **246**, 45-49; (b) T. Kovács and J. Sonnenbichler, *Liebigs Ann-Recl.*, 1997, **1**, 211-212; (c) K. Nozawa, M. Yamada, Y. Tsuda, K. Kawai and S. Nakajima, *Chem. Pharm. Bull.*, 1981, **29**, 2689-2691.
- 16 (a) S. Nakajima, K. Kawai and S. Yamada, *Phytochemistry*, 1976, **15**, 327. (b) T. Kovács, I. Sonnenbichler and J. Sonnenbichler, *Liebigs Ann-Recl.*, 1997, **4**, 773-777.
- 17 (a) Y. Nishimoto, H. Ueda, M. Yasuda, A. Baba, *Chem. Eur. J.*, 2011, **17**, 11135-11138; (b) Y. Nishimoto, R. Moritoh, M. Yasuda and A. Baba, *Angew. Chem. Int. Ed.*, 2009, **48**, 4577-4580.
- 18 For selective examples: (a) H. Wang, Y. Kuang and J. Wu, *Asian J. Org. Chem.*, 2012, **1**, 302-312; (b) E. Tomás-Mendivil, F. C. Heinrich, J.-C. Ortuno, J. Starck and V. Michelet, *ACS Catal.*, 2017, **7**, 380-387.
- 19 Benzopyrylium intermediate in oxymetalation was detected by NMR studies or MS spectra: (a) Y. Zhu and B. Yu, *Chem. Eur. J.*, 2015, **21**, 8771-8780; (b) B. N. Nguyen, L. A. Adrin, E. M. Barreiro, J. B. Brazier, P. Haycock, K. K. Hii, M. Nachtegaal, M. A. Newton and J. Szlachetko, *Organometallics*, 2012, **31**, 2395-2402. Other types of zwitterion intermediate have been characterized by X-ray crystallographic analysis: (c) O. A. Egorova, H. Seo, Y. Kim, D. Moon, Y. M. Rhee and K. H. Ahn, *Angew. Chem. Int. Ed.*, 2011, **50**, 11446-11450; (d) Y. Yu, G. Chen, L. Zhu, Y. Liao, Y. Wu and X. Huang, *J. Org. Chem.*, 2016, **81**, 8142-8154.
- 20 I. Braun, A. M. Asiri and A. S. K. Hashmi, *ACS Catal.*, 2013, **3**, 1902-1907.
- 21 T. M. Baber, G. Qadeer, G. S. Khan, N. H. Rama and W.-Y. Wong, *Acta Cryst.*, 2006, **E62**, o5612-o5613.
- 22 J. D. Forrester, A. Zalkin and D. H. Templeton, *Inorg. Chem.*, 1964, **3**, 63-67.
- 23 S<sub>N</sub>2-type elimination of MeI agrees with inhibition of the elimination step by bulky O-alkyl group in ester moiety (see Table S1 in ESI<sup>†</sup>).
- 24 The values of activation energy of cyclization step shown in Fig. 3 (6-endo: 39.4 kcal/mol, 5-exo: 31.0 kcal/mol) equivalent to two molecules. The activation energy, which equivalents to one molecule, is a half of the values (6-endo: 19.7 kcal/mol, 5-exo: 15.5 kcal/mol).
- 25 (a) A. R. Katritzky, *Chem. Rev.*, 2001, **101**, 1421-1449; (b) P. v. R. Schleyer, C. Maerker, A. Dransfeld, H. Jiao and N. J. R. v. E. Hommes, *J. Am. Chem. Soc.*, 1996, **118**, 6317-6318.
- 26 (a) A. Issaian, D. J. Faizi, J. O. Bailey, P. Mayer, G. Berionni, D. A. Singleton and S. A. Blum, *J. Org. Chem.*, 2017, **82**, 8165-8178; (b) J. Jiang, Z. Zhang and Y. Fu, *Asian J. Org. Chem.*, 2017, **6**, 282-289.
- 27 X. Shi, N. El Hassan, A. Ikni, W. Li, N. Guiblin, A. Spasojević de Biré and N. E. Ghermani, *CrystEngComm.*, 2016, **18**, 3289-3299.
- 28 P. Schwerdtfeger, Atomic Static Dipole Polarizabilities, in Atoms, Molecules and Clusters in Electric Fields, ed. G. Maroulis, Imperial College Press, London, 2006, pp 1-32.
- 29 Silyl anion is stable than carboanion because of the larger atomic radius and higher dipole polarizability of silicon. A. C. Hopkinson and M. H. Lien, *Tetrahedron*, 1981, **37**, 1105-1112.
- 30 K. Zhao, L. Shen, Z.-L. Shen and T.-P. Loh, *Chem. Soc. Rev.*, 2017, **46**, 586-602.
- 31 T.-H. Nguyen, A.-S. Castanet and J. Mortier, *Org. Lett.*, 2006, **8**, 765-768.
- 32 M. Uemura and T. Sakan, *J. Chem. Soc. D*, 1971, **16**, 921.







81x41mm (300 x 300 DPI)

